Bioorganic & Medicinal Chemistry 18 (2010) 5379–5390

Contents lists available at ScienceDirect

Bioorganic & Medicinal Chemistry

journal homepage: www.elsevier.com/locate/bmc

Anti-influenza activity of phenethylphenylphthalimide analogs derived from thalidomide

Yuma Iwai [a,†], Hitoshi Takahashi [b,†], Dai Hatakeyama [a], Kazunori Motoshima [c], Minoru Ishikawa [c], Kazuyuki Sugita [c], Yuichi Hashimoto [c], Yuichi Harada [b], Shigeyuki Itamura [b], Takato Odagiri [b], Masato Tashiro [b], Yoshihisa Sei [d], Kentaro Yamaguchi [d], Takashi Kuzuhara [a,*]

[a] Laboratory of Biochemistry, Faculty of Pharmaceutical Sciences, Tokushima Bunri University, Yamashiro-cho, Tokushima 770-8514, Japan
[b] Center for Influenza Virus Research, National Institute of Infectious Diseases, Gakuen 4-7-1, Musashimurayama-shi, Tokyo 208-0011, Japan
[c] Institute of Molecular & Cellular Biosciences, The University of Tokyo, 1-1-1, Yayoi, Bunkyo-ku, Tokyo 113-0032, Japan
[d] Analytical Chemistry Laboratory, Faculty of Pharmaceutical Sciences at Kagawa Campus, Tokushima Bunri University, Sanuki-City, Kagawa 769-2193, Japan

ARTICLE INFO

Article history:
Received 21 April 2010
Revised 12 May 2010
Accepted 13 May 2010
Available online 20 May 2010

Keywords:
Influenza
Thalidomide
RNA polymerase
Phenethylphenylphthalimide
Endonuclease

ABSTRACT

Swine-origin influenza A virus has caused pandemics throughout the world and influenza A is regarded as a serious global health issue. Hence, novel drugs that will target these viruses are very desirable. Influenza A expresses an RNA polymerase essential for its transcription and replication which comprises PA, PB1, and PB2 subunits. We identified potential novel anti-influenza agents from a screen of 34 synthesized phenethylphenylphthalimide analogs derived from thalidomide (PPT analogs). For this screen we used a PA endonuclease inhibition assay, a PB2 pathogenicity-determinant domain-binding assay, and an anti-influenza A virus assay. Three PPT analogs, PPT-65, PPT-66, and PPT-67, were found to both inhibit PA endonuclease activity and retard the growth of influenza A, suggesting a correlation between their activities. PPT-28 was also found to inhibit the growth of influenza A. These four analogs have a 3,4-dihydroxyphenethyl group in common. We also discuss the possibility that 3,4-dihydroxyphenethyl group flexibility may play an important functional role in PA endonuclease inhibition. Another analog harboring a dimethoxyphenethyl group, PPT-62, showed PB2 pathogenicity-determinant domain-binding activity, but did not inhibit the growth of the virus. Our present results indicate the utility of the PA endonuclease assay in the screening of anti-influenza drugs and are therefore useful for future strategies to develop novel anti-influenza A drugs and for mapping the function of the influenza A RNA polymerase subunits.

1. Introduction

Thalidomide, a hypnotic/sedative drug, was originally launched in the 1950s but was subsequently withdrawn from the market in the 1960s because of its teratogenic properties.[1,2] Thalidomide has been subsequently shown however to be useful in the treatment of Hansen's disease, multiple myeloma, cancer, rheumatoid arthritis, graft-versus-host diseases, and acquired immunodeficiency syndrome.[1–4] Pharmacologically, thalidomide has anti-cachexia, anti-inflammatory, anti-tumor-promoting, anti-angiogenic, tumor cell invasion-inhibiting, anti-viral, and hypoglycemic activities. Hence, thalidomide is a multi-target drug and is thought to be useful as a template in the development of other biologically active compounds. Indeed, Hashimoto and colleagues have previously developed various thalidomide analogs[2,3,5–7] and based on the target molecules have created tumor necrosis factor-production-regulating agents, cyclooxygenase inhibitors, nitric oxide synthase inhibitors, histone deacetylase inhibitors, anti-angiogenic agents, and tubulin polymerization inhibitors.[2,3,5–7] These researchers have also developed the structure of thalidomide based on its pharmacological effects and thereby produced androgen antagonists, progesterone antagonists, cell differentiation inducers, aminopeptidase inhibitors, thymidine phosphorylase inhibitors, μ-calpain inhibitors, α-glucosidase inhibitors, and nuclear liver X receptor antagonists.[2,3,5–7]

In 1918, an influenza A pandemic caused ten million deaths worldwide[8] and strategies to prevent any future expansions of this virus are therefore an important endeavor.[9,10] The avian H5N1 influenza A virus is highly pathogenic to humans[11] and the emer-

Abbreviations: PPT, phenethylphenylphthalimide; IPTG, isopropyl β-D-thiogalactopyranoside; ESI, electrospray ionization; MS, mass spectrometry; FT-ICRMS, Fourier transform ion cyclotron resonance mass spectrometer; MDCK, Madin–Darby canine kidney.

* Corresponding author. Tel.: +81 88 602 8477; fax: +81 88 655 3051.
E-mail address: kuzuhara@ph.bunri-u.ac.jp (T. Kuzuhara).

† These authors contributed equally to this work.

0968-0896/$ - see front matter © 2010 Elsevier Ltd. All rights reserved.
doi:10.1016/j.bmc.2010.05.035

gence of a new strain of this virus in 2009, the swine-origin A/H1N1 pdm influenza virus (SOIV), emphasizes this issue further as it has become a serious global health issue.[12] Although inhibitors of influenza A such as the neuraminidase-like compound oseltamivir are widely used as anti-viral drugs,[13,14] some adverse effects of these agents and also the emergence of viral strains that are resistant to these drugs have now been reported.[15–17]

For the prevention and control of influenza outbreaks, the development of novel anti-viral drugs that are not based on neuraminidase inhibition is now regarded as critical.[12] The influenza A genome consists of a segmented single stranded RNA (−) and its transcription and replication require the activity of a highly conserved RNA-dependent RNA polymerase.[18,19] This polymerase is essential for the influenza A virus to propagate and thus represents a very promising target for anti-viral drug development. The influenza A virus RNA-dependent RNA polymerase is composed of three subunits, PA, PB1, and PB2, and synthesizes viral mRNAs using short capped primers derived from host cellular pre-mRNAs cleaved by the viral endonuclease.[18,19] Yuan et al. and Dias et al. have shown that the N-terminal domain of the PA subunit contains the endonuclease active site and that this domain also harbors RNA/DNA endonuclease activity.[20–22] The PB2 subunit includes K627, which plays a role in the high pathogenicity and host range restriction of the virus.[23–26] We and others have elucidated the tertiary structure of the C-terminal domain (627 domain) of PB2 by X-ray crystallography and identified a unique loop and basic groove proximal to the K627 residue.[27,28] D701 N has also been shown to be associated with the viral pathogenicity levels and is also contained in this domain. Hence, we speculated that the PA endonuclease and PB2 627 domains would be very effective targets in the development of novel anti-influenza A drugs.

Our preliminary results in this regard suggested that phenethylphenylphthalimide (PPT) analogs derived from thalidomide are possible lead compounds (Supplementary Fig. 1) and we thus screened a further cohort of PPT analogs using a PA endonuclease inhibition assay, PB2 627 domain-binding assay and anti-influenza A virus assay. The results of these assays and also of our analysis of the structure–activity relationships of PPT analogs are described.

2. Results

2.1. Synthesis of PPT analogs

PPT derivatives were synthesized as previously described[29] in which diphenylethene derivatives were prepared as *E*/*Z* mixtures via a Wittig reaction of nitrobenzaldehyde with appropriately substituted benzyl ylide (Fig. 1A). After reduction of the nitro group and/or olefin moiety of the adducts, PPT derivatives were obtained by condensation with phthalic anhydride (Fig. 1A). We denoted our PPT analog series as PPT-*n* (*n* = sequential numbering from 1; Fig. 1B). We obtained 37 PPT analogs, three of which (PPT-108, -109, and -112) could not be dissolved in the aqueous assay buffer. We then adopted a strategy for developing a novel anti-influenza A drug which involved two initial in vitro screenings for the inhibition of PA endonuclease activity and a PB2 627 domain-binding assay. After these in vitro selections, we performed an anti-virus assay.

2.2. Inhibition of PA endonuclease by PPT analogs

In the in vitro PA endonuclease assay, we expressed and purified a recombinant PA endonuclease domain (1–220 residues) of the influenza A virus RNA polymerase as previously described.[22] The PA endonuclease domain digests M13mp18 ssDNA in vitro[22] (Fig. 2, lanes 1 and 2) and we examined which of our 34 soluble PPT analogs could inhibit this activity. In the assay, we incubated 0.1 μM of recombinant PA endonuclease domain with both 1 and 10 μM of each PPT analog (Fig. 1B). PPT-65 and PPT-66 significantly inhibited the digestion of M13mp18 at a dose of 10 μM (Fig. 2) and this is the first evidence that agents based on the thalidomide skeleton can inhibit the influenza A virus endonuclease. PPT-67 also showed weak inhibitory activity in this regard but none of the other 31 PPT analogs tested has any effects in the assay (Fig. 2). Interestingly, we found that PPT-65, PPT-66, and PPT-67 all contain a 3,4-dihydroxyphenethyl group (Fig. 1B), indicating that this moiety is important for the inhibition of PA endonuclease (Figs. 1B and 2). A detailed analysis of the structure–function relationships of the PPT analogs is provided later in Section 3.

2.3. Binding of PPT analogs to the PB2 627 domain

As another in vitro selection, we next screened for PB2 627 domain (residues 535–759)-binding factors among PPT analogs. This domain has been reported to be associated with viral pathogenicity and host range restriction,[25–28] and we speculated that it would play an important role and that any chemical that bound to this domain would have anti-viral effects. We established an assay system to detect the PB2 627 domain protein by ESI-MS.[30,31] In this analysis, molecular weights are presented as a number divided by the charge number, which in the case of the PB2 627 domain is 25146. As shown in Figure 3A, peaks with sodium adducts appeared with the mass to charge (*m*/*z*), which corresponds to the molecular weight of the PB2 627 domain (Fig. 2A). We thus concluded that these peaks are derived from an intact PB2 627 domain protein. We next mixed and analyzed 1–3 μM of PB2 627 domain protein with 50 μM of each PPT analog to detect whether binding occurred. When PB2 627 domain mixed with PPT-62 (Fig. 3F), additional peaks other than the PB2 627 domain were appeared. The differences of *m*/*z* values between additional peaks and those derived from PB2 627 domain were 43.0 and 42.7 (Fig. 3F). When multiplied by nine, these values become 387 and 384 which are almost same as the molecular weight of PPT-62 (387). In case of the other charge, especially e = 8, shifted peaks were also observed (Supplementary Fig. 2). This indicates that PPT-62 directly associates with the PB2 627 domain. No binding was observed for several other PPT analogs (Fig. 3B–G), indicating that the association of PPT-62 and PB2 627 is specific. Two kinds of bound form of PB2 627 domain, (PB2 627 domain + PPT-62) and (PB2 627 domain + two PPT-62), were observed indicating that two molecules of PPT-62 bind to this domain. This may be because two PPT-62 molecules interact with each other via π–π bonding because this chemical contains an aromatic ring.

2.4. Inhibition of influenza A by PPT analogs

We performed an influenza A virus assay in a cell culture system for the four PPT analogs that selected by these two in vitro assays (PPT-62, -65, -66, and -67), and also include one further PPT analog (PPT-28) containing a 3,4-dihydroxyphenethyl group, and additional analogs (PPT-68 and -125) for comparison. MDCK cells undergo cytopathy following infection by influenza A in culture and we used this system to examine whether our selected PPT analogs could inhibit growth of this virus. Various concentrations (0.63–80 μM) of each PPT analog and 100 $TCID_{50}$ (50% of the infectious dose) of influenza A virus were premixed, and then added to the culture medium of the MDCK cells. We performed this assay three times and thereby determined the viability of the MDCK cells (Fig. 4). DMSO alone did not inhibit the viral growth whereas PPT-65 and -66 did so at a dose of around 40 μM (Fig. 4). PPT-67 also exerted these effects, but was more toxic to the cells (Supplementary Fig. 3). This is the first evidence that compounds with a

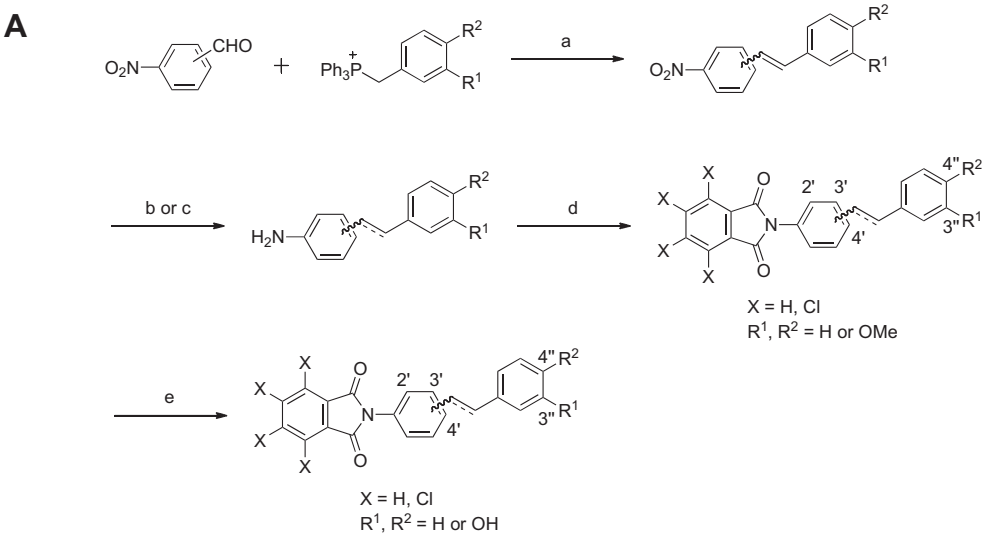

B

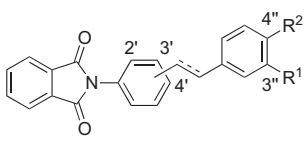

Compound	position	single (s) or double bond (d)	R^1	R^2
PPT2P	2'	s	H	H
PPT62	2'	s	OMe	OMe
PPT65	2'	s	OH	OH
PPT63	3'	s	OMe	OMe
PPT66	3'	s	OH	OH
PPT21	4'	s	H	H
PPT32	4'	s	OMe	OMe
PPT108	4'	d	H	H
PPT113	4'	d	OH	OH
PPT121	4'	s	OMe	H
PPT123	4'	s	H	OMe
PPT125	4'	s	OH	H
PPT137	4'	s	H	OH

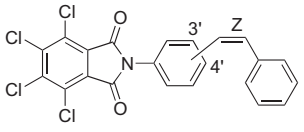

Compound	position
PPT86	3'
PPT87	4'

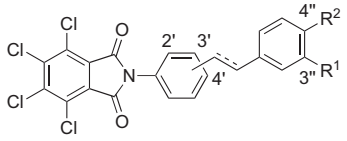

Compound	position	single (s) or double bond (d)	R^1	R^2
PPT43	2'	s	H	H
PPT59	2'	s	OMe	OMe
PPT67	2'	s	OH	OH
PPT61	3'	s	H	H
PPT60	3'	s	OMe	OMe
PPT68	3'	s	OH	OH
PPT22	4'	s	H	H
PPT27	4'	s	OMe	OMe
PPT28	4'	s	OH	OH
PPT84	3'	d	H	H
PPT95	3'	d	OMe	OMe
PPT97	3'	d	OH	OH
PPT109	4'	d	H	H
PPT112	4'	d	OMe	OMe
PPT91	3'	s	OMe	H
PPT80	3'	s	H	OMe
PPT94	3'	s	OH	H
PPT85	3'	s	H	OH
PPT122	4'	s	OMe	H
PPT124	4'	s	H	OMe
PPT136	4'	s	OH	H
PPT138	4'	s	H	OH

Figure 1. (A) Scheme of the chemical synthesis of PPT analogs. Reagents and conditions: (a) K_2CO_3, 18-crown-6, CH_2Cl_2, reflux; (b) H_2, 10%, Pd/C, EtOAc, rt; (c) $SnCl_2{\cdot}2H_2O$, EtOAc, reflux; (d) phthalic anhydride or tetrachlorophthalic anhydride, neat, 200 °C; (e) BBr_3, CH_2Cl_2, 0 °C. (B) Chemical structures of the synthesized PPT analogs screened for anti-influenza A activities.

phthalimide skeleton derived from thalidomide possess anti-influenza A virus activity. PPT-62, -68, and -125 did not inhibit the viral growth (Fig. 4) nor inhibit PA endonuclease activity (Fig. 2). Hence, a correlation exists between the inhibition of PA endonuclease and inhibition of influenza A. Interestingly, we also found that PPT-28, which contains a 3,4-dihydroxyphenethyl group, inhibits the influenza virus but not via the targeting of the PA endonuclease. Table 1 lists the EC_{50} and CC_{50} values for these analogs which were calculated from the data shown in Figure 4. The average EC_{50} for PPT-28, -65, and -66 was 24, 48, and 26 μM, and the CC_{50} of PPT-28 and -65 was above 80 μM, respectively. These compounds are therefore putative candidate anti-influenza A drugs themselves and may also have utility as seeds for the development of such agents.

3. Discussion

We demonstrate that three PPT analogs, PPT-65, PPT-66, and PPT-67, inhibit PA endonuclease and the viral growth. Significantly,

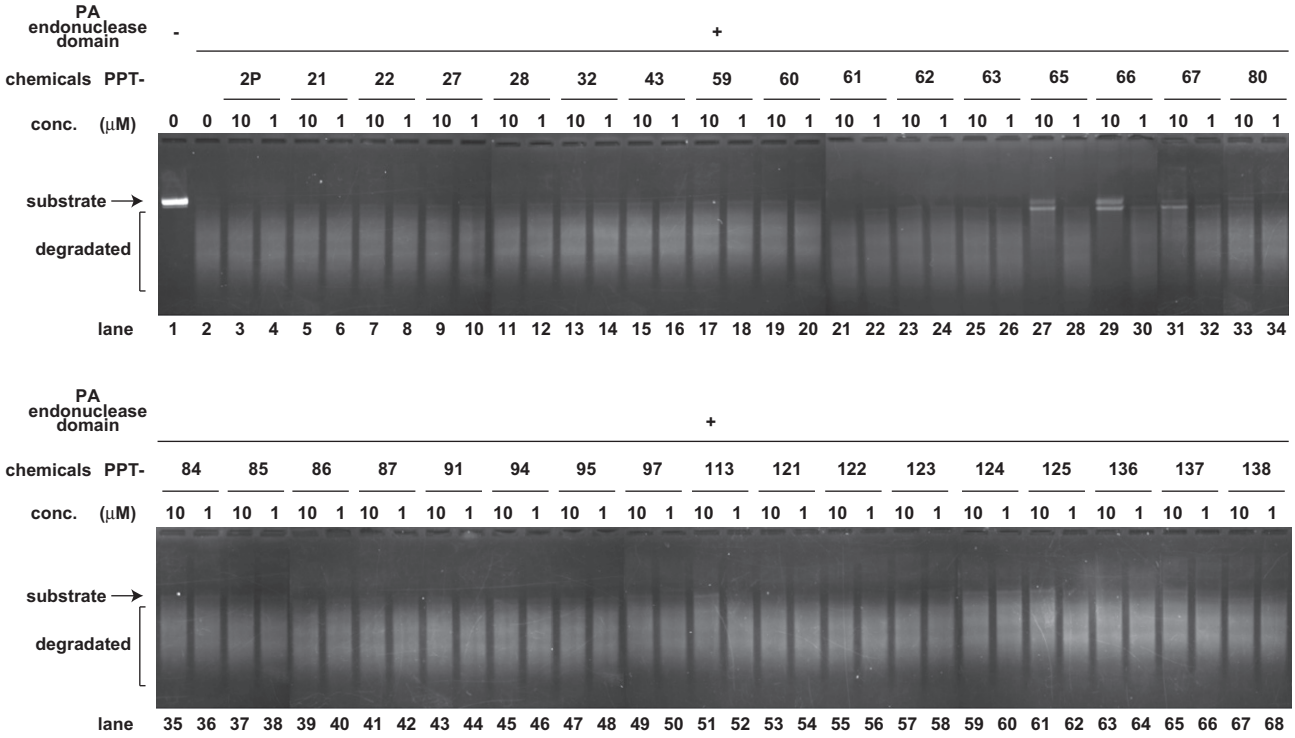

Figure 2. Screening of PPT analogs for anti-influenza A activity using a PA endonuclease assay. Effects of various PPT analogs upon the endonuclease activity of the N-terminal domain of the PA subunit of influenza A virus RNA-dependent RNA polymerase. The recombinant N-terminal domain of PA was added to each reaction at 0.35 μg/100 μl. A zero control (no PA domain added) was also assayed. PPT analogs were added at 1 or 10 μM and M13mp18 was used as the substrate.

all of these analogs contain a 3,4-dihydroxyphenethyl group at the *ortho* or *meta* position of the *N*-phenyl moiety (Fig. 1B). The PPT analogs possessing methoxyphenethyl group(s) (PPT-27, -32, -59, -60, -62, -63, -80, -91, -95, -121, -122, -123, and -124), a monohydroxyphenethyl group (PPT-85, -94, -125, -136, -137, and -138) or an unsubstituted phenethyl group (PPT-21, -22, -43, -61, -84, -86, -87 and PPT2P) (Fig. 1B) did not inhibit PA endonuclease activity (Fig. 2). This suggests a central functional role of the 3,4-dihydroxyphenethyl moiety for this inhibition. Previously, we have reported that catechins[32] can inhibit PA endonuclease[22] and it has been shown also that these molecules have anti-influenza activity.[33] Significantly, the catechins also contain a 3,4-dihydroxyphenyl group (Supplementary Fig. 4), confirming that this moiety plays a role in the inhibition of PA endonuclease and in suppressing the growth of influenza (Fig. 5).

PPT-28 possesses a 3,4-dihydroxyphenethyl group at the *para* position (Fig. 1B) and does not inhibit PA endonuclease (Fig. 2), indicating that introduction of 3,4-dihydroxyphenethyl group into the '*ortho* or *meta*' position of the *N*-phenyl moiety be critical for this activity. Moreover, conversion of the 3,4-dihydroxyphenethyl group to a 3,4-dihydroxycinnamyl group, that is, as seen for PPT-97 and -113 (Fig. 1B), results in the loss of PA endonuclease-inhibitory activity (Fig. 2), also indicating the importance of the flexible 3,4-dihydroxyphenethyl group for this process. A freely rotating 3,4-dihydroxyphenyl group might also play an important functional role in this process. In combination with the importance of the position (*ortho* or *meta* of the *N*-phenyl moiety) at which the 3,4-dihydroxyphenethyl group is introduced, the spatial position of the two hydroxyl groups of the 3,4-dihydroxyphenethyl moiety in the molecule seem also to be critical for this activity. PPT-68 has a 3,4-dihydroxyphenethyl group but shows little or no inhibition of PA endonuclease (data not shown). We suggest therefore that the four chloride groups introduced into the phthalimide moiety inhibit or weaken this activity as PPT-67 also possesses a tetrachlorophthalimide group and shows weaker inhibition than PPT-65 or PPT-66 (Figs. 1 and 2). Although we have not yet investigated other functional groups derived from catechin, that is, 3,4,5-trihydroxyphenethyl and/or 3,5-dihydroxyphenethyl groups among others, our current results indicate that the development of chemicals with a 3,4-dihydroxyphenethyl group will likely produce more effective PA endonuclease inhibitors and better anti-influenza A drugs.

PPT-62 binds to the PB2 pathogenicity-determining 627 domain and harbors a dimethoxyphenethyl group (Figs. 1B and 3). In contrast, PPT-21 and PPT-43 do not possess a dimethoxyphenethyl group (Fig. 1B) and did not show binding to this domain (Fig. 3). PPT-62 is very similar to PPT-67 except for a methoxy group (Fig. 1B) but as PPT-67 binds only weakly to the PB2 627 domain (Fig. 3), the dimethoxy group of PPT-62 is likely to be important for this domain-binding. PPT-59 is identical to PPT-62 other than four additional chlorides (Fig. 1B) and also binds only weakly to the PB2 627 domain (Fig. 3), suggesting that these chlorides inhibit this binding. Based on these results, the development of compounds possessing a dimethoxyphenethyl group will likely lead to the production of drugs with a higher affinity for the PB2 627 domain.

Our current data show that PPT analogs can be used as tools to investigate the functional roles of influenza A virus RNA polymerase domains. Based on our results (summarized in Fig. 6), the PB2 pathogenicity-determinant domain may have a regulatory function rather than an essential one. Also, the correlation between the inhibition of PA endonuclease and suppression of the influenza A virus confirmed the importance of this enzyme for viral growth. Our results also indicate that the PA endonuclease assay is a useful screening tool for novel anti-influenza A drugs as the information obtained correlates well with virus

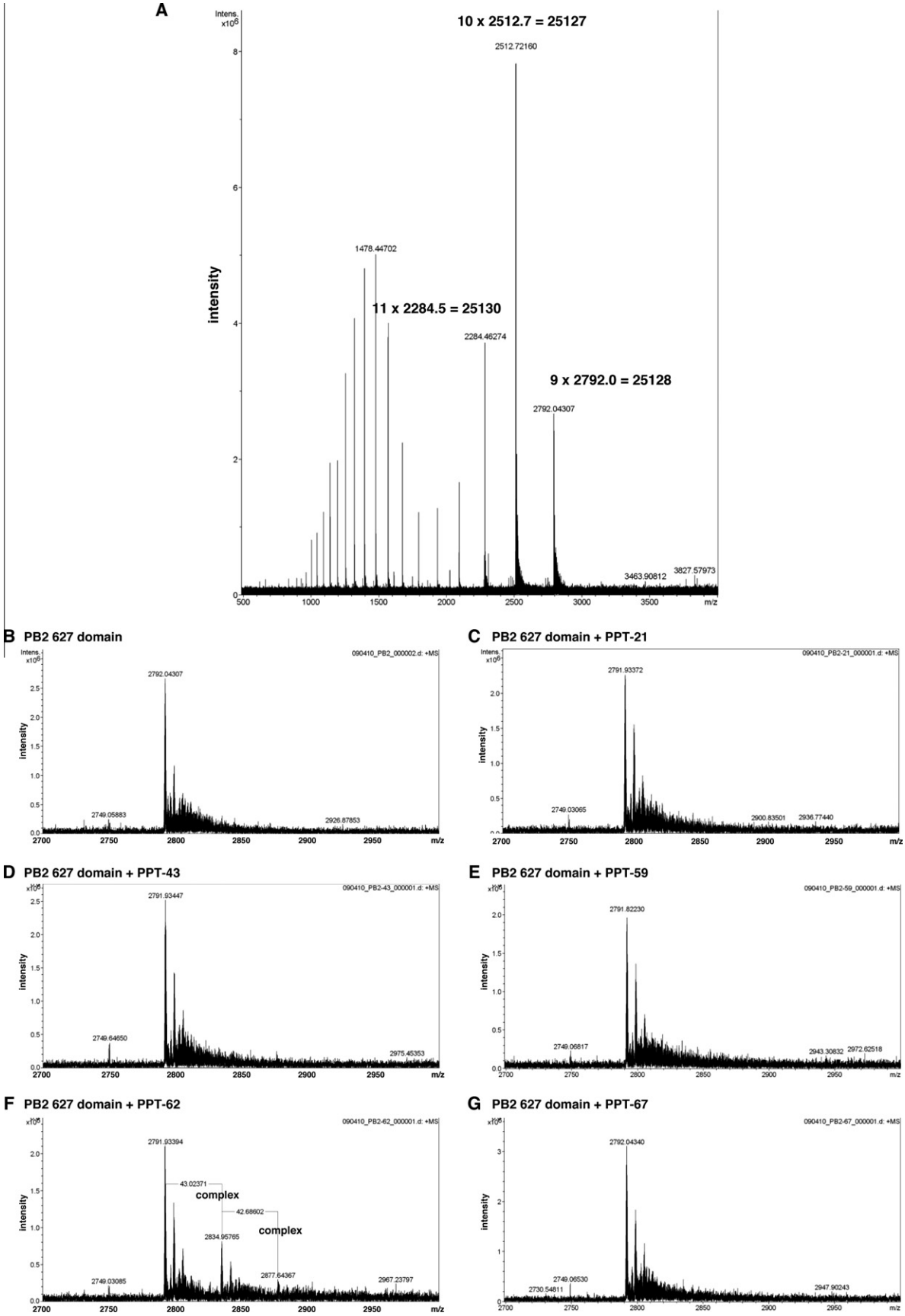

Figure 3. (A) Establishment of a detection system for factors that bind to the PB2 627 domain protein using FT-ICRMS. Vertical axis shows the intensity of the protein peaks. The horizontal axis indicates the m/z values. (B–G) Binding of PPT analogs to the PB2 627 domain. Direct binding analysis of PPT analogs to the PB2 627 domain using FT-ICRMS. The PB2 627 domain and PPT analogs were mixed and applied to FT-ICRMS. The vertical axis shows the intensity of the peaks. The horizontal axis indicates the m/z values. (B) PB2 627 domain only. The PB2 627 domain was also incubated with (C) PPT-21; (D) PPT-43; (E) PPT-59; (F) PPT-62 and (G) PPT-67.

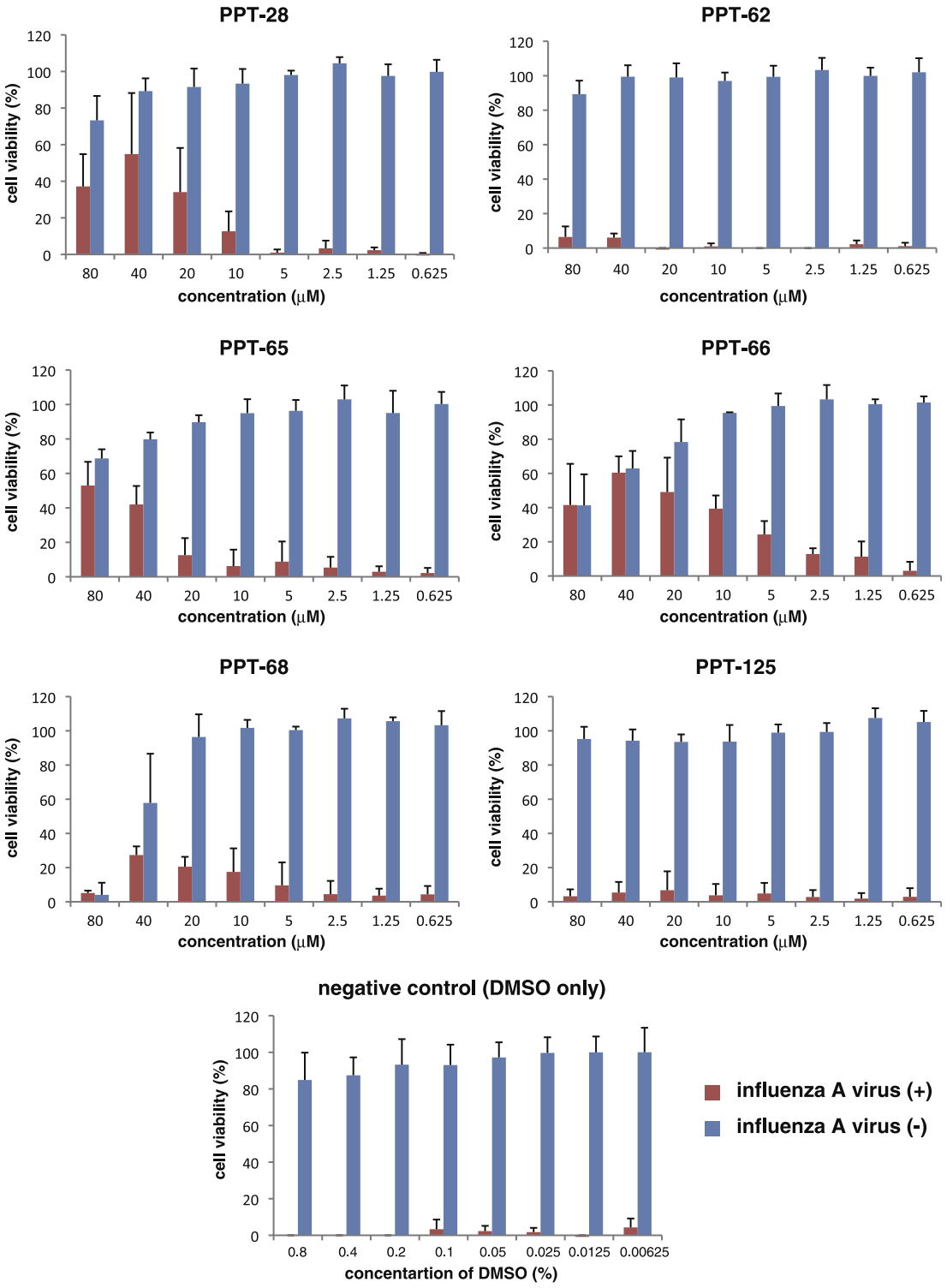

Figure 4. Inhibition of influenza A viral growth by PPT analogs. MDCK cells were treated with (red bar) or without (blue bar) influenza A virus. The cells were then treated with various concentrations of PPT analogs (0.63–80 μM), some of which suppressed viral-induced cell death. DMSO was used as the PPT solvent. The vertical and horizontal axes indicate cell viability (%) and the concentration of PPT analogs, respectively. Experiments were performed in triplicate, and the average values with standard deviations are indicated.

growth and this method is easier and thus more convenient to perform than other screening approaches using the virus itself. The effective doses of PPT analogs are high at present, but as the tertiary structures of the PA endonuclease and PB2 627 domains have already been determined,[20,21,27,28] docking simulations in silico[34] can be used for the further development and optimization of these compounds. We conclude finally that the chemical and biochemical information presented herein will be

Table 1
EC_{50} and CC_{50} values for the anti-influenza A activities of the indicated PPT analogs

Virus (μM)	DMSO		PPT-28		PPT-62		PPT-65		PPT-66		PPT-68		PPT-125	
	(+) EC_{50}	(−) CC_{50}	(+) EC_{50}	(−) CC_{50}	(+) EC_{50}	(−) CC_{50}	(+) EC_{50}	(−) CC_{50}	(+) EC_{50}	(−) CC_{50}	(+) EC_{50}	(−) CC_{50}	(+) EC_{50}	(−) CC_{50}
1st	>80	>80	30	>80	>80	>80	60	>80	28	>80	>80	62	>80	>80
2nd	>80	>80	25	>80	>80	>80	37	>80	11	48	>80	34	>80	>80
3rd	>80	>80	16	>80	>80	>80	>80[a]	>80	40	57	>80	37	>80	>80
Average	>80	>80	24	>80	>80	>80	48[b]	>80	26	nd	>80	44	>80	>80

The EC_{50} and CC_{50} (μM) values were estimated from a dose-dependent curve in Figure 4.
nd, not determined.
[a] The EC_{40} was around 50 (μM). The EC_{50} was not estimated due to the low viability of the cells exposed to this higher dose. The shapes of the curves calculated for the three experiments are similar as shown in Supplementary Figure 5.
[b] Average was calculated from the first and second experiments in this case. See Supplementary Figure 5.

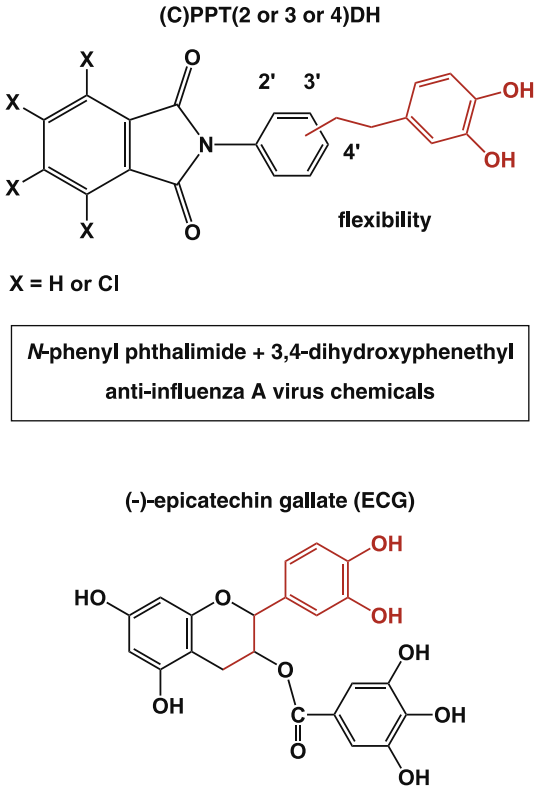

Figure 5. Consensus structure for the PPT analogs possessing anti-influenza A activity. The 3,4-dihydroxyphenyl group is characteristic of catechin molecules (shown as red) which also inhibit the influenza virus.

very useful for the future development of novel drugs against the influenza A virus.

4. Experimental

4.1. Synthesis of PPT analogs

Synthesis of the PPT analogs is described in the text and depicted also in Figure 1A. Their chemical structures are depicted in Figure 1B.

4.1.1. *N*-(2-(2-Phenylethyl)phenyl)phthalimide: PPT2P

Mp 90.8–91.2 °C. ^{1}H NMR (500 MHz, $CDCl_3$) δ: 7.94–7.98 (m, 2H), 7.78–7.82 (m, 2H), 7.40 (dt, 1H, J = 7.5, 1.5 Hz), 7.33–7.37 (m 2H), 7.16–7.22 (m, 3H), 7.10–7.15 (m 1H), 7.04–7.08 (m, 2H), 2.78–2.89 (m, 4H). Anal. Calcd for $C_{22}H_{17}NO_2$: C, 80.71; H, 5.23; N, 4.28. Found: C, 80.85; H, 5.36; N, 4.20.

4.1.2. *N*-(4-(2-Phenylethyl)phenyl)phthalimide: PPT-21

Mp 216.5–218.0 °C. ^{1}H NMR (500 MHz, $CDCl_3$) δ: 7.96 (dd, 2H, J = 5.5, 3.1 Hz), 7.50 (dd, 2H, J = 5.5, 3.1 Hz), 7.36–7.29 (m, 6H), 7.23–7.19 (m, 3H), 3.01–2.94 (m, 4H). FAB-MS m/z: 327 $[M]^+$, 328 $[M+H]^+$. Anal. Calcd for $C_{22}H_{17}NO_2$: C, 80.71; H, 5.23; N, 4.28. Found: C, 80.71; H, 5.53; N, 4.27.

4.1.3. 4,5,6,7-Tetrachloro-*N*-[4-(2-phenylethyl)phenyl]phthalimide: PPT-22

Mp 222.0–223.0 °C. ^{1}H NMR (500 MHz, $CDCl_3$) δ: 7.33–7.28 (m, 6H), 7.22–7.19 (m, 3H), 3.00–2.98 (m, 2H), 2.97–2.94 (m, 2H). FAB-MS m/z: 463 $[M]^+$, 464 $[M+H]^+$, 465 $[M+2]^+$, 466 $[M+3]^+$, 467 $[M+4]^+$, 468 $[M+5]^+$. Anal. Calcd for $C_{22}H_{13}Cl_4NO_2$: C, 56.81; H, 2.82; N, 3.01. Found: C, 56.85; H, 3.02; N, 2.94.

4.1.4. 4,5,6,7-Tetrachloro-*N*-{4-[2-(3,4-dimethoxyphenyl)ethyl]phenyl}phthalimide: PPT-27

Mp 220.0–221.5 °C. ^{1}H NMR (500 MHz, $CDCl_3$) δ: 7.28 (s, 4H), 6.78 (d, 1H, J = 8.5 Hz), 6.71 (dd, 1H, J = 8.5, 1.8 Hz), 6.62 (d, 1H, J = 1.8 Hz), 3.85 (s, 3H), 3.82 (s, 3H), 2.96–2.93 (m, 2H), 2.90–2.87 (m, 2H). FAB-MS m/z: 523 $[M]^+$, 524 $[M+H]^+$, 525 $[M+2]^+$, 526 $[M+3]^+$, 527 $[M+4]^+$, 528 $[M+5]^+$. HRMS (FAB) calcd for $C_{24}H_{17}Cl_4NO_4$ 522.9912; found: 522.9929 $(M)^+$.

4.1.5. 4,5,6,7-Tetrachloro-*N*-{4-[2-(3,4-dihydroxyphenyl)ethyl]phenyl}phthalimide: PPT-28

Mp 260.0–263.0 °C. ^{1}H NMR (500 MHz, DMSO-d_6) δ: 8.70 (s, 1H), 8.62 (s, 1H), 7.38 (d, 2H, J = 8.5 Hz), 7.30 (d, 2H, J = 8.5 Hz), 6.64 (d, 1H, J = 2.1 Hz), 6.62 (d, 1H, J = 7.9 Hz), 6.47 (dd, 1H, J = 7.9, 2.1 Hz), 2.88–2.85 (m, 2H), 2.75–2.72 (m, 2H). FAB-MS m/z: 495 $[M]^+$, 496 $[M+H]^+$, 497 $[M+2]^+$, 498 $[M+3]^+$, 499 $[M+4]^+$, 500 $[M+5]^+$. Anal. Calcd for $C_{22}H_{13}Cl_4NO_4 \cdot 1/3H_2O$: C, 52.52; H, 2.74; N, 2.78. Found: C, 52.47; H, 2.85; N, 2.51.

4.1.6. *N*-{4-[2-(3,4-Dimethoxyphenyl)ethyl]phenyl}phthalimide: PPT-32

Mp 180.0–181.0 °C. ^{1}H NMR (500 MHz, $CDCl_3$) δ: 7.94 (dd, 2H, J = 5.5, 3.1 Hz), 7.77 (dd, 2H, J = 5.5, 3.1 Hz), 7.33–7.28 (m, 4H), 6.79 (d, 1H, J = 7.9 Hz), 6.73 (dd, 1H, J = 7.9, 1.8 Hz), 6.63 (d, 1H, J = 1.8 Hz), 3.85 (s, 3H), 3.82 (s, 3H), 2.95–2.92 (m, 2H), 2.90–2.87 (m, 2H). FAB-MS m/z: 387 $[M]^+$, 388 $[M+H]^+$. Anal. Calcd for $C_{24}H_{21}NO_4 \cdot 1/5H_2O$: C, 73.72; H, 5.52; N, 3.58. Found: C, 73.98; H, 5.44; N, 3.64.

4.1.7. 4,5,6,7-Tetrachloro-*N*-[2-(2-phenylethyl)phenyl]phthalimide: PPT-43

Mp 148.0–149.0 °C. ^{1}H NMR (500 MHz, $CDCl_3$) δ: 7.42–7.39 (m, 1H), 7.35–7.32 (m, 2H), 7.19–7.16 (m, 2H), 7.14–7.09 (m, 2H), 7.06 (d, 2H, J = 6.7 Hz), 2.87–2.84 (m, 2H), 2.78–2.75 (m, 2H). FAB-MS m/z: 463 $[M]^+$, 464 $[M+H]^+$, 465 $[M+2]^+$, 466 $[M+3]^+$, 467 $[M+4]^+$,

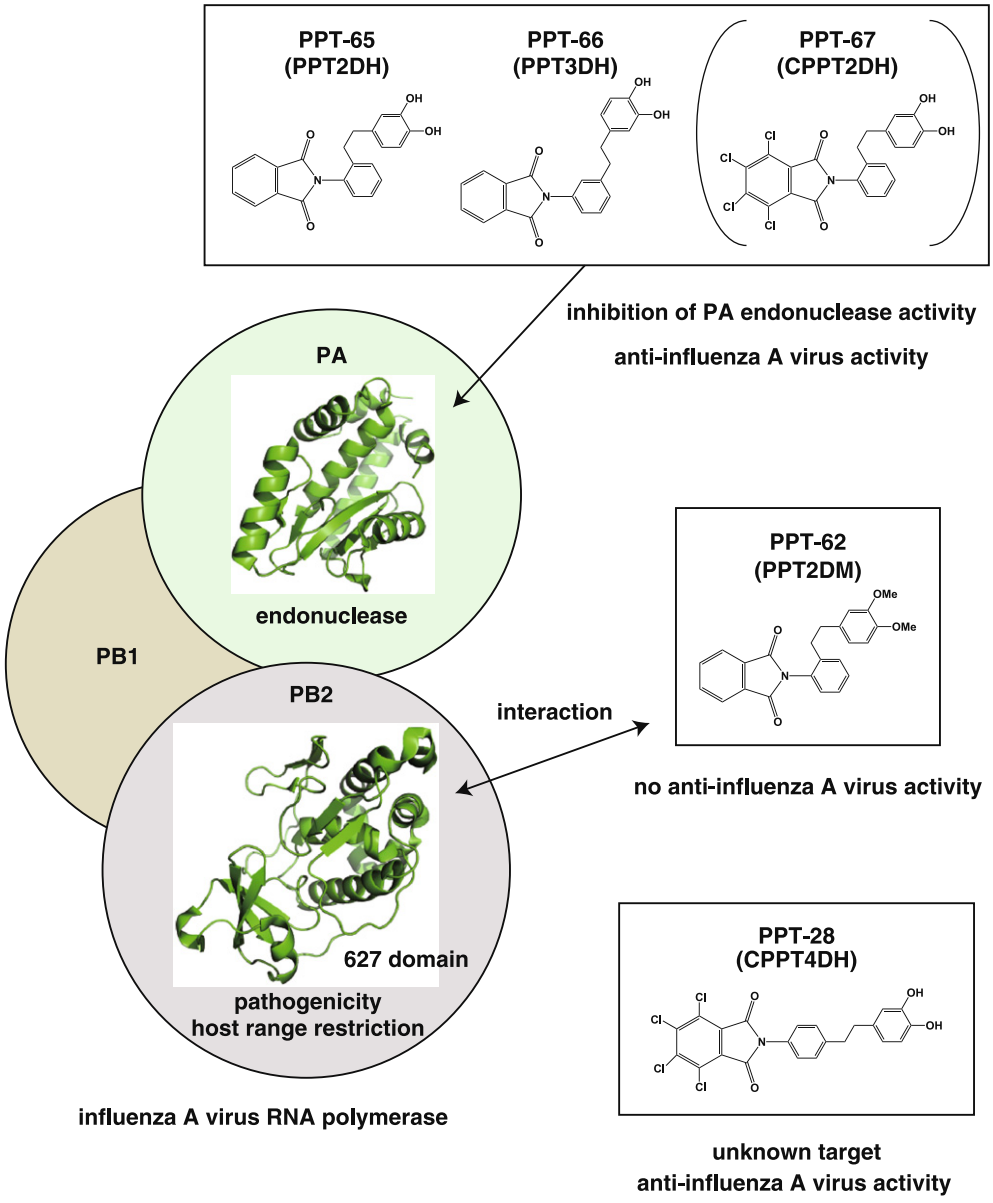

Figure 6. The functional domains of influenza A virus RNA polymerase mapped with respect to their interaction with the PPT analogs. PPT-65, -66, and -67 inhibit PA endonuclease activity and have anti-influenza A virus activity. PPT-62 binds to the PB2 pathogenicity-determinant 627 domain. PPT-28 has anti-influenza A virus activity. Structure–function relationship analysis indicates that the 3,4-dihydroxyphenethyl group is important for the anti-influenza A activity of these analogs.

468 $[M+5]^+$. Anal. Calcd for $C_{22}H_{13}Cl_4NO_2$: C, 56.81; H, 2.82; N, 3.01. Found: C, 56.67; H, 2.92; N, 2.94.

4.1.8. 4,5,6,7-Tetrachloro-*N*-{2-[2-(3, 4-dimethoxyphenyl)ethyl] phenyl}phthalimide: PPT-59

Mp 157.0–158.0 °C. ^{1}H NMR (500 MHz, $CDCl_3$) δ: 7.41 (td, 1H, J = 7.9, 1.8 Hz), 7.35 (td, 1H, J = 7.9, 1.8 Hz), 7.32 (dd, 1H, J = 7.3, 1.8 Hz), 7.15 (dd, 1H, J = 7.9, 1.8 Hz), 6.68 (d, 1H, J = 7.9 Hz), 6.61 (dd, 1H, J = 7.9, 1.8 Hz), 6.53 (d, 1H, J = 1.8 Hz), 3.81 (s, 3H), 3.75 (s, 3H), 2.80 (s, 4H). FAB-MS m/z: 523 $[M]^+$, 524 $[M+H]^+$, 525 $[M+2]^+$, 526 $[M+3]^+$, 527 $[M+4]^+$, 528 $[M+5]^+$. Anal. Calcd for $C_{24}H_{17}Cl_4NO_4$: C, 54.88; H, 3.26; N, 2.67. Found: C, 54.63; H, 3.37; N, 2.54.

4.1.9. 4,5,6,7-Tetrachloro-*N*-{3-[2-(3,4-dimethoxyphenyl)ethyl] phenyl}phthalimide: PPT-60

Mp 166.0–167.0 °C. ^{1}H NMR (500 MHz, $CDCl_3$) δ: 7.43–7.39 (m, 1H), 7.24–7.20 (m, 3H), 6.79 (d, 1H, J = 7.9 Hz), 6.71 (dd, 1H, J = 7.9, 1.8 Hz), 6.64 (d, 1H, J = 1.8 Hz), 3.86 (s, 3H), 3.83 (s, 3H), 2.97–2.94 (m, 2H), 2.91–2.88 (m, 2H). FAB-MS m/z: 523 $[M]^+$, 524 $[M+H]^+$, 525 $[M+2]^+$, 526 $[M+3]^+$, 527 $[M+4]^+$, 528 $[M+5]^+$. Anal. Calcd for $C_{24}H_{17}Cl_4NO_4 \cdot 1/4H_2O$: C, 54.42; H, 3.33; N, 2.64. Found: C, 54.49; H, 3.36; N, 2.61.

4.1.10. 4,5,6,7-Tetrachloro-*N*-[3-(2-phenylethyl)phenyl]phthalimide: PPT-61

Mp 187.0–187.5 °C. ^{1}H NMR (500 MHz, $CDCl_3$) δ: 7.42 (t, 1H, J = 7.9 Hz), 7.29 (t, 2H, J = 7.9 Hz), 7.26–7.25 (m, 1H), 7.24 (dd, 2H, J = 7.9, 1.8 Hz), 7.20 (dd, 1H, J = 7.9, 1.2 Hz), 7.19 (d, 2H, J = 7.9 Hz), 3.00–2.97 (m, 2H), 2.96–2.94 (m, 2H). FAB-MS m/z: 463 $[M]^+$, 464 $[M+H]^+$, 465 $[M+2]^+$, 466 $[M+3]^+$, 467 $[M+4]^+$, 468 $[M+5]^+$. Anal. Calcd for $C_{22}H_{13}Cl_4NO_2$: C, 56.81; H, 2.82; N, 3.01. Found: C, 56.66; H, 2.91; N, 2.95.

4.1.11. *N*-{2-[2-(3,4-Dimethoxyphenyl)ethyl]phenyl}phthalimide: PPT-62

Mp 103.0–105.0 °C. ^{1}H NMR (500 MHz, $CDCl_3$) δ: 7.95 (dd, 2H, J = 5.5, 3.1 Hz), 7.80 (dd, 2H, J = 5.5, 3.1 Hz), 7.41–7.37 (m, 1H),

7.37–7.33 (m, 1H), 7.31 (dd, 1H, *J* = 7.3, 1.8 Hz), 7.20 (dd, 1H, *J* = 7.3, 1.8 Hz), 6.69 (d, 1H, *J* = 7.9 Hz), 6.59 (dd, 1H, *J* = 7.9, 1.8 Hz), 6.50 (d, 1H, *J* = 1.8 Hz), 3.80 (s, 3H), 3.68 (s, 3H), 2.79 (s, 4H). FAB-MS *m*/*z*: 387 $[M]^+$, 388 $[M+H]^+$. Anal. Calcd for $C_{24}H_{21}NO_4$: C, 74.40; H, 5.46; N, 3.62. Found: C, 74.34; H, 5.59; N, 3.55.

4.1.12. *N*-{3-[2-(3,4-Dimethoxyphenyl)ethyl]phenyl} phthalimide: PPT-63

Mp 132.5–133.5 °C. ^{1}H NMR (500 MHz, $CDCl_3$) δ: 7.96 (dd, 2H, *J* = 5.5, 3.1 Hz), 7.80 (dd, 2H, *J* = 5.5, 3.1 Hz), 7.43–7.39 (m, 1H), 7.28–7.26 (m, 2H), 7.19 (d, 1H, *J* = 7.3 Hz), 6.80 (d, 1H, *J* = 7.9 Hz), 6.73 (dd, 1H, *J* = 7.9, 1.8 Hz), 6.65 (d, 1H, *J* = 1.8 Hz), 3.85 (s, 3H), 3.83 (s, 3H), 2.99–2.95 (m, 2H), 2.93–2.89 (m, 2H). FAB-MS *m*/*z*: 387 $[M]^+$, 388 $[M+H]^+$. Anal. Calcd for $C_{24}H_{21}NO_4$: C, 74.40; H, 5.46; N, 3.62. Found: C, 74.33; H, 5.49; N, 3.54.

4.1.13. *N*-{2-[2-(3,4-Dihydroxyphenyl)ethyl]phenyl}phthal imide: PPT-65

Mp 63.0–65.0 °C. ^{1}H NMR (500 MHz, $CDCl_3$) δ: 7.95 (dd, 2H, *J* = 5.5, 2.4 Hz), 7.81 (dd, 2H, *J* = 5.5, 2.4 Hz), 7.41–7.38 (m, 1H), 7.36–7.31 (m, 2H), 7.18 (dd, 1H, *J* = 7.9, 1.2 Hz), 6.66 (d, 1H, *J* = 7.9 Hz), 6.52 (d, 1H, *J* = 1.8 Hz), 6.49 (dd, 1H, *J* = 7.9, 1.8 Hz), 5.16 (s, 1H), 5.00 (s, 1H), 2.76 (m, 4H). FAB-MS *m*/*z*: 359 $[M]^+$, 360 $[M+H]^+$. HRMS (FAB) calcd for $C_{22}H_{17}NO_4$ 359.1158; found: 359.1127 $(M)^+$.

4.1.14. *N*-{3-[2-(3,4-Dihydroxyphenyl)ethyl]phenyl}phthal imide: PPT-66

Mp 171.5–172.0 °C. ^{1}H NMR (500 MHz, $CDCl_3$) δ: 7.96 (dd, 2H, *J* = 5.5, 2.4 Hz), 7.81 (dd, 2H, *J* = 5.5, 2.4 Hz), 7.42 (t, 1H, *J* = 7.9 Hz), 7.23 (dd, 1H, *J* = 7.9, 2.4 Hz), 7.22 (dd, 1H, *J* = 7.9, 1.8 Hz), 7.13 (m, 1H), 6.78 (d, 1H, *J* = 7.9 Hz), 6.63 (dd, 1H, *J* = 7.9, 1.8 Hz), 6.56 (d, 1H, *J* = 1.8 Hz), 5.66 (s, 1H), 5.16 (s, 1H), 2.94–2.90 (m, 2H), 2.86–2.83 (m, 2H). FAB-MS *m*/*z*: 359 $[M]^+$, 360 $[M+H]^+$. Anal. Calcd for $C_{22}H_{17}NO_4$: C, 73.53; H, 4.77; N, 3.90. Found: C, 73.24; H, 4.84; N, 3.83.

4.1.15. 4,5,6,7-Tetrachloro-*N*-{2-[2-(3,4-dihydroxyphenyl) ethyl]phenyl}phthalimide: PPT-67

Mp 227.0–229.5 °C. ^{1}H NMR (500 MHz, $CDCl_3$) δ: 7.41 (m, 1H), 7.36–7.32 (m, 2H), 7.14–7.13 (m, 1H), 6.66 (d, 1H, *J* = 7.9 Hz), 6.53 (d, 1H, *J* = 2.4 Hz), 6.49 (dd, 1H, *J* = 7.9, 1.8 Hz), 5.09 (s, 1H), 4.94 (s, 1H), 2.76 (s, 4H). FAB-MS *m*/*z*: 495 $[M]^+$, 496 $[M+H]^+$, 497 $[M+2]^+$, 498 $[M+3]^+$, 499 $[M+4]^+$, 500 $[M+5]^+$. Anal. Calcd for $C_{22}H_{13}Cl_4NO_4$: C, 53.15; H, 2.64; N, 2.82. Found: C, 53.03; H, 2.88; N, 2.62.

4.1.16. 4,5,6,7-Tetrachloro-*N*-{3-[2-(3,4-dihydroxyphenyl) ethyl]phenyl}phthalimide: PPT-68

Mp 208.0–210.0 °C. ^{1}H NMR (500 MHz, $CDCl_3$) δ: 7.43 (t, 1H, *J* = 7.9 Hz), 7.24 (d, 1H, *J* = 7.3 Hz), 7.20 (m, 1H), 7.10 (s, 1H), 6.78 (d, 1H, *J* = 7.9 Hz), 6.63 (dd, 1H, *J* = 7.9, 1.8 Hz), 6.58 (d, 1H, *J* = 1.8 Hz), 5.53 (s, 1H), 5.15 (s, 1H), 2.93–2.91 (m, 2H), 2.85–2.82 (m, 2H). FAB-MS *m*/*z*: 495 $[M]^+$, 496 $[M+H]^+$, 497 $[M+2]^+$, 498 $[M+3]^+$, 499 $[M+4]^+$, 500 $[M+5]^+$. Anal. Calcd for $C_{22}H_{13}Cl_4NO_4 \cdot 2/3H_2O$: C, 51.90; H, 2.84; N, 2.75. Found: C, 51.70; H, 3.03; N, 2.60.

4.1.17. 4,5,6,7-Tetrachloro-*N*-{3-[2-(4-methoxyphenyl) ethyl]phenyl}phthalimide: PPT-80

Mp 169.0–170.0 °C. ^{1}H NMR (500 MHz, $CDCl_3$) δ: 7.41 (t, 1H, *J* = 8.5 Hz), 7.23–7.22 (m, 2H), 7.09 (d, 2H, *J* = 8.5 Hz), 6.83 (d, 2H, *J* = 8.5 Hz), 3.79 (s, 3H), 2.96–2.93 (m, 2H), 2.91–2.87 (m, 2H). FAB-MS *m*/*z*: 494 $[M+H]^+$, 495 $[M+2]^+$, 496 $[M+3]^+$, 497 $[M+4]^+$, 498 $[M+5]^+$. Anal. Calcd for $C_{23}H_{15}Cl_4NO_3 \cdot 1/4H_2O$: C, 55.28; H, 3.13; N, 2.80. Found: C, 55.28; H, 3.09; N, 2.78.

4.1.18. 4,5,6,7-Tetrachloro-*N*-{3-[(1*E*)-2-phenylethenyl] phenyl}phthalimide: PPT-84

Mp 259.5–261.5 °C. ^{1}H NMR (500 MHz, $CDCl_3$) δ: 7.58–7.56 (m, 2H), 7.52–7.49 (m, 3H), 7.37 (t, 2H, *J* = 7.9 Hz), 7.31–7.28 (m, 2H), 7.15 (d, 1H, *J* = 16.8 Hz), 7.12 (d, 1H, *J* = 16.8 Hz). FAB-MS *m*/*z*: 461 $[M]^+$, 462 $[M+H]^+$, 463 $[M+2]^+$, 464 $[M+3]^+$, 465 $[M+4]^+$, 466 $[M+5]^+$. Anal. Calcd for $C_{22}H_{11}Cl_4NO_2 \cdot 1/3H_2O$: C, 56.32; H, 2.51; N, 2.99. Found: C, 56.55; H, 2.56; N, 2.98.

4.1.19. 4,5,6,7-Tetrachloro-*N*-{3-[2-(4-hydroxyphenyl) ethyl]phenyl}phthalimide: PPT-85

Mp 210.0–212.0 °C. ^{1}H NMR (500 MHz, $CDCl_3$) δ: 7.41 (t, 1H, *J* = 7.3 Hz), 7.24–7.20 (m, 3H), 7.03 (d, 2H, *J* = 8.5 Hz), 6.75 (d, 2H, *J* = 8.5 Hz), 4.60 (br s, 1H), 2.95–2.92 (m, 2H), 2.89–2.86 (m, 2H). FAB-MS *m*/*z*: 479 $[M]^+$, 480 $[M+H]^+$, 481 $[M+2]^+$, 482 $[M+3]^+$, 483 $[M+4]^+$, 484 $[M+5]^+$. Anal. Calcd for $C_{22}H_{13}Cl_4NO_3$: C, 54.92; H, 2.72; N, 2.91. Found: C, 54.68; H, 2.82; N, 2.83.

4.1.20. 4,5,6,7-Tetrachloro-*N*-{3-[(1*Z*)-2-phenylethenyl] phenyl}phthalimide: PPT-86

White powder from CH_2Cl_2/*n*-hexane. Mp 164.0–165.5 °C. ^{1}H NMR (500 MHz, $CDCl_3$) δ: 7.37–7.26 (m, 5H), 7.25–7.18 (m, 4H), 6.67 (d, 1H, *J* = 12.2 Hz), 6.59 (d, 1H, *J* = 12.2 Hz). FAB-MS *m*/*z*: 461 $[M]^+$, 462 $[M+H]^+$, 463 $[M+2]^+$, 464 $[M+3]^+$, 465 $[M+4]^+$, 466 $[M+5]^+$. Anal. Calcd for $C_{22}H_{11}Cl_4NO_2$: C, 57.05; H, 2.39; N, 3.02. Found: C, 56.81; H, 2.53; N, 2.93.

4.1.21. 4,5,6,7-Tetrachloro-*N*-{4-[(1*Z*)-2-phenylethenyl] phenyl}phthalimide: PPT-87

White powder from CH_2Cl_2/*n*-hexane. Mp 155.5–157.5 °C. ^{1}H NMR (500 MHz, $CDCl_3$) δ: 7.58–7.49 (m, 1H), 7.38–7.18 (m, 8H), 6.67 (d, 1H, *J* = 12.8 Hz), 6.59 (d, 1H, *J* = 12.8 Hz). FAB-MS *m*/*z*: 461 $[M]^+$, 462 $[M+H]^+$, 463 $[M+2]^+$, 464 $[M+3]^+$, 465 $[M+4]^+$, 466 $[M+5]^+$. Anal. Calcd for $C_{22}H_{11}Cl_4NO_2 \cdot 1/3H_2O$: C, 56.32; H, 2.51; N, 2.99. Found: C, 56.35; H, 2.60; N, 2.96.

4.1.22. 4,5,6,7-Tetrachloro-*N*-{3-[2-(3-methoxyphenyl) ethyl]phenyl}phthalimide: PPT-91

Mp 150.0–151.0 °C. ^{1}H NMR (500 MHz, $CDCl_3$) δ: 7.42 (t, 1H, *J* = 7.9 Hz), 7.26–7.25 (m, 2H), 7.23 (m, 1H), 7.20 (t, 1H, *J* = 7.9 Hz), 6.78 (d, 1H, *J* = 7.3 Hz), 6.75 (dd, 1H, *J* = 7.9, 1.8 Hz), 6.72–6.72 (m, 1H), 3.78 (s, 3H), 3.00–2.96 (m, 2H), 2.94–2.91 (m, 2H). FAB-MS *m*/*z*: 493 $[M]^+$, 494 $[M+H]^+$, 495 $[M+2]^+$, 496 $[M+3]^+$, 497 $[M+4]^+$, 498 $[M+5]^+$. Anal. Calcd for $C_{23}H_{15}Cl_4NO_3 \cdot 1/4H_2O$: C, 55.28; H, 3.13; N, 2.80. Found: C, 55.43; H, 3.11; N, 2.82.

4.1.23. 4,5,6,7-Tetrachloro-*N*-{3-[2-(3-hydroxyphenyl) ethyl]phenyl}phthalimide: PPT-94

Mp 213.0–215.0 °C. ^{1}H NMR (500 MHz, $CDCl_3$) δ: 7.42 (t, 1H, *J* = 7.9 Hz), 7.25–7.20 (m, 3H), 7.15 (t, 1H, *J* = 7.9 Hz), 6.76 (d, 1H, *J* = 7.9 Hz), 6.68 (dd, 1H, *J* = 7.9, 2.4 Hz), 6.62 (t, 1H, *J* = 1.8 Hz), 2.98–2.95 (m, 2H), 2.92–2.88 (m, 2H). FAB-MS *m*/*z*: 479 $[M]^+$, 480 $[M+H]^+$, 481 $[M+2]^+$, 482 $[M+3]^+$, 483 $[M+4]^+$, 484 $[M+5]^+$. Anal. Calcd for $C_{22}H_{13}Cl_4NO_3$: C, 54.92; H, 2.72; N, 2.91. Found: C, 54.68; H, 2.99; N, 2.77.

4.1.24. 4,5,6,7-Tetrachloro-*N*-{3-[(1*E*)-2-(3,4-dimethoxyphenyl) ethenyl]phenyl}phthalimide: PPT-95

Mp 248.0–249.0 °C. ^{1}H NMR (500 MHz, $CDCl_3$) δ: 7.56–7.54 (m, 2H), 7.49 (t, 1H, *J* = 7.9 Hz), 7.29–7.27 (m, 1H), 7.09 (d, 1H, *J* = 16.2 Hz), 7.07–7.05 (m, 2H), 6.99 (d, 1H, *J* = 16.2 Hz), 6.87 (d, 1H, *J* = 7.9 Hz), 3.95 (s, 3H), 3.91 (s, 3H). FAB-MS *m*/*z*: 521 $[M]^+$, 522 $[M+H]^+$, 523 $[M+2]^+$, 524 $[M+3]^+$, 525 $[M+4]^+$, 526 $[M+5]^+$. Anal. Calcd for $C_{24}H_{15}Cl_4NO_4 \cdot 1/2H_2O$: C, 54.16; H, 3.03; N, 2.63. Found: C, 53.98; H, 3.03; N, 2.49.

4.1.25. 4,5,6,7-Tetrachloro-*N*-{3-[(1*E*)-2-(3,4-dihydroxyphenyl) ethenyl]phenyl}phthalimide: PPT-97

Mp 257.0–260.0 °C. ^{1}H NMR (500 MHz, $CDCl_3$) δ: 7.51 (dt, 1H, J = 7.9, 1.2 Hz), 7.50 (m, 1H), 7.47 (t, 1H, J = 7.9 Hz), 7.26–7.25 (m, 1H), 7.05 (d, 1H, J = 1.8 Hz), 7.00 (d, 1H, J = 16.5 Hz), 6.95 (dd, 1H, J = 8.5, 1.8 Hz), 6.91 (d, 1H, J = 16.5 Hz), 6.85 (d, 1H, J = 8.5 Hz), 5.59 (br s, 1H), 5.54 (br s, 1H). FAB-MS m/z: 493 $[M]^+$, 494 $[M+H]^+$, 495 $[M+2]^+$, 496 $[M+3]^+$, 497 $[M+4]^+$, 498 $[M+5]^+$. HRMS (FAB) calcd for $C_{22}H_{11}Cl_4NO_4$ 492.9442; found: 492.9467 $(M)^+$.

4.1.26. *N*-{4-[(1*E*)-2-Phenylethenyl]phenyl}phthalimide: PPT-108

Mp 297.0–299.0 °C. ^{1}H NMR (500 MHz, $CDCl_3$) δ: 7.97 (dd, 2H, J = 5.5, 3.1 Hz), 7.81 (dd, 2H, J = 5.5, 3.1 Hz), 7.65 (d, 2H, J = 8.5 Hz), 7.54 (d, 2H, J = 7.9 Hz), 7.46 (d, 2H, J = 8.5 Hz), 7.38 (t, 2H, J = 7.9 Hz), 7.28 (tt, 1H, J = 7.9, 1.2 Hz), 7.15 (s, 2H). FAB-MS m/z: 325 $[M]^+$, 326 $[M+H]^+$. Anal. Calcd for $C_{22}H_{15}NO_2 \cdot 1/3H_2O$: C, 79.74; H, 4.77; N, 4.23. Found: C, 79.50; H, 4.69; N, 4.19.

4.1.27. 4,5,6,7-Tetrachloro-*N*-{4-[(1*E*)-2-phenylethenyl] phenyl}phthalimide: PPT-109

Mp 296.0–296.5 °C. ^{1}H NMR (500 MHz, $CDCl_3$) δ: 7.65 (d, 2H, J = 8.5 Hz), 7.54 (d, 2H, J = 7.3 Hz), 7.42 (d, 2H, J = 8.5 Hz), 7.38 (t, 2H, J = 7.3 Hz), 7.29 (tt, 1H, J = 7.3, 1.2 Hz), 7.17 (d, 1H, J = 16.5 Hz), 7.13 (d, 1H, J = 16.5 Hz). FAB-MS m/z: 461 $[M]^+$, 462 $[M+H]^+$, 463 $[M+2]^+$, 464 $[M+3]^+$, 465 $[M+4]^+$, 466 $[M+5]^+$. Anal. Calcd for $C_{22}H_{11}Cl_4NO_2$: C, 57.05; H, 2.39; N, 3.02. Found: C, 56.83; H, 2.69; N, 3.09.

4.1.28. 4,5,6,7-Tetrachloro-*N*-{4-[(1*E*)-2-(3,4-dimethoxyphenyl) ethenyl]phenyl}phthalimide: PPT-112

Mp 281.0–284.0 °C. ^{1}H NMR (500 MHz, $CDCl_3$) δ: 7.62 (d, 2H, J = 8.5 Hz), 7.40 (d, 2H, J = 8.5 Hz), 7.11 (d, 1H, J = 16.2 Hz), 7.09–7.05 (m, 2H), 7.00 (d, 1H, J = 16.2 Hz), 6.88 (d, 1H, J = 8.5 Hz), 3.96 (s, 3H), 3.91 (s, 3H). FAB-MS m/z: 521 $[M]^+$, 522 $[M+H]^+$, 523 $[M+2]^+$, 524 $[M+3]^+$, 525 $[M+4]^+$, 526 $[M+5]^+$. Anal. Calcd for $C_{24}H_{15}Cl_4NO_4 \cdot 1/2H_2O$: C, 54.16; H, 3.03; N, 2.63. Found: C, 54.24; H, 2.97; N, 2.55.

4.1.29. *N*-{4-[(1*E*)-2-(3,4-Dihydroxyphenyl)ethenyl]phenyl} phthalimide: PPT-113

Mp 278.0–281.0 °C. ^{1}H NMR (500 MHz, DMSO-d_6) δ: 7.97 (dd, 2H, J = 5.5, 3.1 Hz), 7.90 (dd, 2H, J = 5.5, 3.1 Hz), 7.67 (d, 2H, J = 8.5 Hz), 7.40 (d, 2H, J = 8.5 Hz), 7.14 (d, 1H, J = 16.2 Hz), 7.01 (d, 1H, J = 2.4 Hz), 6.97 (d, 1H, J = 16.2 Hz), 6.89 (dd, 1H, J = 8.5, 1.8 Hz), 6.73 (d, 1H, J = 7.9 Hz). FAB-MS m/z: 357 $[M]^+$, 358 $[M+H]^+$. Anal. Calcd for $C_{22}H_{15}NO_4 \cdot 1/4H_2O$: C, 73.02; H, 4.32; N, 3.87. Found: C, 73.21; H, 4.36; N, 3.91.

4.1.30. *N*-{4-[2-(3-Methoxyphenyl)ethyl]phenyl}phthalimide: PPT-121

Mp 127.0–127.5 °C. ^{1}H NMR (500 MHz, $CDCl_3$) δ: 7.96 (dd, 2H, J = 5.5, 3.1 Hz), 7.79 (dd, 2H, J = 5.5, 3.1 Hz), 7.36–7.32 (m, 4H), 7.22 (t, 1H, J = 7.9 Hz), 6.82 (d, 1H, J = 7.3 Hz), 6.76 (dd, 1H, J = 7.3, 1.8 Hz), 6.74 (d, 1H, J = 1.8 Hz), 3.79 (s, 3H), 3.00–2.96 (m, 2H), 2.95–2.91 (m, 2H). FAB-MS m/z: 357 $[M]^+$, 358 $[M+H]^+$. Anal. Calcd for $C_{23}H_{19}NO_3 \cdot 1/4H_2O$: C, 76.33; H, 5.43; N, 3.87. Found: C, 76.34; H, 5.40; N, 3.87.

4.1.31. 4,5,6,7-Tetrachloro-*N*-{4-[2-(3-methoxyphenyl) ethyl]phenyl}phthalimide: PPT-122

Mp 170.5–172.0 °C. ^{1}H NMR (500 MHz, $CDCl_3$) δ: 7.34–7.29 (m, 4H), 7.22 (t, 1H, J = 7.9 Hz), 6.80 (d, 1H, J = 7.3 Hz), 6.76 (dd, 1H, J = 7.9, 1.8 Hz), 6.73 (s, 1H), 3.79 (s, 3H), 3.00–2.97 (m, 2H), 2.95–2.91 (m, 2H). FAB-MS m/z: 493 $[M]^+$, 494 $[M+H]^+$, 495 $[M+2]^+$, 496 $[M+3]^+$, 497 $[M+4]^+$, 498 $[M+5]^+$. HRMS (FAB) calcd for $C_{23}H_{15}Cl_4NO_3$ 492.9806; found: 492.9834 $(M)^+$.

4.1.32. *N*-{4-[2-(4-Methoxyphenyl)ethyl]phenyl}phthalimide: PPT-123

Mp 196.5–199.0 °C. ^{1}H NMR (500 MHz, $CDCl_3$) δ: 7.96 (dd, 2H, J = 5.5, 3.1 Hz), 7.79 (dd, 2H, J = 5.5, 3.1 Hz), 7.35 (d, 2H, J = 9.2 Hz), 7.32 (d, 2H, J = 8.5 Hz), 7.13 (d, 2H, J = 8.5 Hz), 6.85 (d, 2H, J = 9.2 Hz), 3.80 (s, 3H). FAB-MS m/z: 357 $[M]^+$, 358 $[M+H]^+$. Anal. Calcd for $C_{23}H_{19}NO_3$: C, 77.29; H, 5.36; N, 3.92. Found: C, 77.21; H, 5.51; N, 3.83.

4.1.33. 4,5,6,7-Tetrachloro-*N*-{4-[2-(4-methoxyphenyl)ethyl] phenyl}phthalimide: PPT-124

Mp 209.5–211.5 °C. ^{1}H NMR (500 MHz, $CDCl_3$) δ: 7.30 (s, 4H), 7.10 (d, 2H, J = 8.5 Hz), 6.84 (d, 2H, J = 8.5 Hz), 3.80 (s, 3H), 2.96–2.93 (m, 2H), 2.91–2.90 (m, 2H). FAB-MS m/z: 494 $[M+H]^+$, 495 $[M+2]^+$, 496 $[M+3]^+$, 497 $[M+4]^+$, 498 $[M+5]^+$. Anal. Calcd for $C_{23}H_{15}Cl_4NO_3$: C, 55.79; H, 3.05; N, 2.83. Found: C, 55.43; H, 3.20; N, 2.76.

4.1.34. *N*-{4-[2-(3-Hydroxyphenyl)ethyl]phenyl}phthalimide: PPT-125

Mp 229.0–232.0 °C. ^{1}H NMR (500 MHz, $CDCl_3$) δ: 7.96 (dd, 2H, J = 5.5, 3.1 Hz), 7.80 (dd, 2H, J = 5.5, 3.1 Hz), 7.35–7.30 (m, 4H), 7.17 (t, 1H, J = 7.9 Hz), 6.80 (d, 1H, J = 7.3 Hz), 6.68 (dd, 1H, J = 7.9, 2.4 Hz), 6.60 (s, 1H), 2.98–2.95 (m, 2H), 2.92–2.89 (m, 2H). FAB-MS m/z: 343 $[M]^+$, 344 $[M+H]^+$. Anal. Calcd for $C_{22}H_{17}NO_3 \cdot 1/5H_2O$: C, 76.15; H, 5.05; N, 4.04. Found: C, 76.38; H, 5.24; N, 4.05.

4.1.35. 4,5,6,7-Tetrachloro-*N*-{4-[2-(3-hydroxyphenyl) ethyl]phenyl}phthalimide: PPT-136

Mp 267.0–268.0 °C. ^{1}H NMR (500 MHz, DMSO-d_6) δ: 9.25 (br s, 1H), 7.40 (d, 2H, J = 7.9 Hz), 7.31 (d, 2H, J = 7.9 Hz), 7.06 (t, 1H, J = 7.3 Hz), 6.67 (d, 1H, J = 7.3 Hz), 6.66 (s, 1H), 6.58 (d, 1H, J = 7.3 Hz), 2.92–2.90 (m, 2H), 2.84–2.81 (m, 2H). FAB-MS m/z: 479 $[M]^+$, 480 $[M+H]^+$, 481 $[M+2]^+$, 482 $[M+3]^+$, 483 $[M+4]^+$, 484 $[M+5]^+$. HRMS (FAB) calcd for $C_{22}H_{13}Cl_4NO_3$ 478.9650; found: 478.9694 $(M)^+$.

4.1.36. *N*-{4-[2-(4-Hydroxyphenyl)ethyl]phenyl}phthalimide: PPT-137

Mp 285.0–288.0 °C. ^{1}H NMR (500 MHz, $CDCl_3$) δ: 7.96 (dd, 2H, J = 5.5, 3.1 Hz), 7.80 (dd, 2H, J = 5.5, 3.1 Hz), 7.35–7.30 (m, 4H), 7.08 (d, 2H, J = 7.9 Hz), 6.77 (d, 2H, J = 8.5 Hz), 2.94–2.92 (m, 2H), 2.90–2.88 (m, 2H). FAB-MS m/z: 343 $[M]^+$, 344 $[M+H]^+$. Anal. Calcd for $C_{22}H_{17}NO_3 \cdot 1/2H_2O$: C, 74.99; H, 5.15; N, 3.97. Found: C, 74.97; H, 5.20; N, 3.89.

4.1.37. 4,5,6,7-Tetrachloro-*N*-{4-[2-(4-hydroxyphenyl) ethyl]phenyl}phthalimide: PPT-138

Mp 266.0–268.0 °C. ^{1}H NMR (500 MHz, DMSO-d_6) δ: 9.15 (br s, 1H), 7.37 (d, 2H, J = 8.5 Hz), 7.30 (d, 2H, J = 8.5 Hz), 7.03 (d, 2H, J = 8.5 Hz), 6.66 (d, 2H, J = 8.5 Hz), 2.89–2.86 (m, 2H), 2.81–2.78 (m, 2H). FAB-MS m/z: 479 $[M]^+$, 480 $[M+H]^+$, 481 $[M+2]^+$, 482 $[M+3]^+$, 483 $[M+4]^+$, 484 $[M+5]^+$. Anal. Calcd for $C_{22}H_{13}Cl_4NO_3$: C, 54.92; H, 2.72; N, 2.91. Found: C, 54.60; H, 3.00; N, 2.82.

4.2. Expression and purification of the PA endonuclease and PB2 627 domain proteins

The influenza (A/PR/8/34) H1N1 RNA polymerase PA and PB2 plasmids, pBMSA-PA and pBMSA-PB2, were sourced from the DNA Bank, Riken BioResource Center (Tsukuba, Japan; originally deposited by Dr. Susumu Nakada).[35] The cDNA fragment corresponding to the PA N-terminal endonuclease domain (residues

1–220) was amplified by PCR[36] from pBMSA-PA using the primers PA endonuclease forward NdeI, GCCGTTCATATGGAAGATTTTG TGCGACAA and PA endonuclease reverse BamHI, GCCGTTGGATCCT ATTGGTCGGCAAGCTTGCG. A cDNA fragment of the PB2 627 domain (residues 535–759, previously denoted as the PB2 3/3 domain[28]) was amplified by PCR from pBMSA-PB2 using the following primers: PB2 Met 627, GCCGTTCATATGATGTGGGAGATTAA TGGT and PB2 stop BamHI, GCCGTTGGATCCTTAATTGATGGCCA TCCGAAT. These two amplified products were then subcloned into the pET28a(+) plasmid (Novagen, Madison, WI) at the NdeI and BamHI restriction sites. The two resulting constructs were then introduced into BL21-CodonPlus (Stratagene, La Jolla, CA) *Escherichia coli* cells. The induction of 6x his-tagged recombinant protein expression from these constructs were achieved by the addition of isopropyl β-D-thiogalactopyranoside (IPTG)[37] to TBG-M9 medium and this was followed by purification using Ni^{2+}-agarose.[38] The recombinant PA endonuclease domain protein was further purified to near homogeneity using a HiTrap™ Q FF column (GE Healthcare, Buckinghamshire, UK) with the Akta™ prime plus system (GE Healthcare). For further purification of the PB2 627 domain, the his-tagged proteins were cleaved by thrombin and purified using a HiTrap™ CM FF column (GE Healthcare) also with the Akta™ prime plus system.

4.3. PA endonuclease activity assay

Influenza A RNA polymerase PA endonuclease activity assays were performed essentially as described by Dias et al.[20–22] with some modifications. Briefly, we modified the pH conditions (from 8.0 to 7.3) and used 1 μg of M13mp18 single stranded circular phage DNA as the assay substrate. We added 0.35 μg of recombinant N-terminal endonuclease domain of the PA subunit to 100 μl of assay buffer in each reaction (the final concentration of the protein was about 0.1 μM). PPT analogs were then added to the reaction and products were analyzed by agarose electrophoresis and stained with ethidium bromide.

4.4. Electrospray ionization (ESI) mass spectrometry (MS)

Chemicals at a dose of 50 μM and recombinant PB2 627 domain protein at 1–3 μM were mixed in 200 μl of 10 mM ammonium acetate/methanol (1:1), to which 1% acetic acid was added. This mixture was then injected at 100 μl/h into an ESI-MS.[30,31] For binding analysis, recombinant PB2 627 domain protein was used.[28] Measurements were performed with a Fourier transform ion cyclotron resonance mass spectrometer (FT-ICRMS, Bruker Daltonics), equipped with an ESI ion source, using the following parameters: capillary −4.0 kV, spray shield −3.5 kV, dry temp 40 °C, resolution at m/z 2792 50 k, flow rate 100 μl/h, solvent 10 mM ammonium acetate buffer 49.5%, methanol 49.5%, and acetic acid 1% (v/v/v).

4.5. Inhibition of viral growth

Madin–Darby canine kidney (MDCK) cells[39] were cultured in MEM (Minimum Essential Medium; Gibco/Invitrogen, Carlsbad, CA) supplemented with 10% fetal bovine serum in 5% CO_2 incubator at 37 °C. A confluent monolayer of MDCK cells was prepared in each well of a 96-well plate. Various concentrations (0.63–80 μM) of PPT analogs were mixed with or without 100 $TCID_{50}$ (50% of the infectious dose) of H1N1 influenza A virus (A/Puerto Rico/8/34 (PR8)) in the presence of trypsin and incubated at 37 °C for 30 min.[40] MDCK cells were washed with PBS(−) and the viral mixture was added to the cells. Treated cells were then incubated for four days at 34 °C under 5% CO_2. After incubation, the medium was removed and cells were fixed with a 10% formaldehyde solution. Viable cells were stained with NB solution (0.1% naphthol blue black, 0.1% sodium acetate, and 9% acetic acid) and the OD_{630} was measured.[40] Cell viability was calculated based on a calibration of the OD_{630} values observed in mock-infected and virus-only wells as 100% and 0%, respectively.

Acknowledgments

The influenza virus (A/PR/8/34) RNA polymerase PA and PB2 plasmids, pBMSA-PA and pBMSA-PB2, were provided by the DNA Bank, RIKEN BioResource Center (Tsukuba, Japan; originally deposited by Dr. Susumu Nakada) with the support of National Bio-Resources Project of the Ministry of Education, Culture, Sports, Science and Technology, Japan (MEXT). This work was supported in part by a Grant-in-Aid for Young Scientists (Start-up) 20870037 (D.H.) from the Japan Society for the Promotion of Science (JSPS), Japan.

Supplementary data

Supplementary data associated with this article can be found, in the online version, at doi:10.1016/j.bmc.2010.05.035.

References and notes

1. Bartlett, J. B.; Dredge, K.; Dalgleish, A. G. *Nat. Rev. Cancer* **2004**, *4*, 314.
2. Hashimoto, Y. *Bioorg. Med. Chem.* **2002**, *10*, 461.
3. Hashimoto, Y. *Curr. Med. Chem.* **1998**, *5*, 163.
4. Hideshima, T.; Chauhan, D.; Shima, Y.; Raje, N.; Davies, F. E.; Tai, Y. T.; Treon, S. P.; Lin, B.; Schlossman, R. L.; Richardson, P.; Muller, G.; Stirling, D. I.; Anderson, K. C. *Blood* **2000**, *96*, 2943.
5. Hashimoto, Y. *Arch. Pharm. Weinheim* **2008**, *341*, 536.
6. Hashimoto, Y. *Mini-Rev. Med. Chem.* **2002**, *2*, 543.
7. Hashimoto, Y.; Tanatani, A.; Nagasawa, K.; Miyachi, H. *Drugs Future* **2004**, *29*, 383.
8. Taubenberger, J. K.; Reid, A. H.; Lourens, R. M.; Wang, R.; Jin, G.; Fanning, T. G. *Nature* **2005**, *437*, 889.
9. Morse, S. S. *Nat. Med.* **2007**, *13*, 681.
10. Horimoto, T.; Kawaoka, Y. *Nat. Rev. Microbiol.* **2005**, *3*, 591.
11. Hatta, M.; Gao, P.; Halfmann, P.; Kawaoka, Y. *Science* **2001**, *293*, 1840.
12. Neumann, G.; Noda, T.; Kawaoka, Y. *Nature* **2009**, *459*, 931.
13. De Clercq, E. *Nat. Rev. Drug Disc.* **2006**, *5*, 1015.
14. Hayden, F. G.; Atmar, R. L.; Schilling, M.; Johnson, C.; Poretz, D.; Paar, D.; Huson, L.; Ward, P.; Mills, R. G. N. *N. Eng. J. Med.* **1999**, *341*, 1336.
15. Reece, P. A. *J. Med. Virol.* **2007**, *79*, 1577.
16. Collins, P. J.; Haire, L. F.; Lin, Y. P.; Liu, J.; Russell, R. J.; Walker, P. A.; Skehel, J. J.; Martin, S. R.; Hay, A. J.; Gamblin, S. J. *Nature* **2008**, *453*, 1258.
17. Izumi, Y.; Tokuda, K.; O'dell, K. A.; Zorumski, C. F.; Narahashi, T. *Neurosci. Lett.* **2007**, *426*, 54.
18. Honda, A.; Ishihama, A. *Biol. Chem.* **1997**, *378*, 483.
19. Honda, A.; Mizumoto, K.; Ishihama, A. *Proc. Natl. Acad. Sci. U.S.A.* **2002**, *99*, 13166.
20. Yuan, P.; Bartlam, M.; Lou, Z.; Chen, S.; Zhou, J.; He, X.; Lv, Z.; Ge, R.; Li, X.; Deng, T.; Fodor, E.; Rao, Z.; Liu, Y. *Nature* **2009**, *458*, 909.
21. Dias, A.; Bouvier, D.; Crépin, T.; McCarthy, A. A.; Hart, D. J.; Baudin, F.; Cusack, S.; Ruigrok, R. W. *Nature* **2009**, *458*, 914.
22. Kuzuhara, T.; Iwai, Y.; Takahashi, H.; Hatakeyama, D.; Echigo, N. *PLoS Curr. Influenza* **2009**. RRN1052.
23. Subbarao, E. K.; London, W.; Murphy, B. R. *J. Virol.* **1993**, *67*, 1761.
24. Shinya, K.; Hamm, S.; Hatta, M.; Ito, H.; Ito, T.; Kawaoka, Y. *Virology* **2004**, *320*, 258.
25. Labadie, K.; Dos Santos Afonso, E.; Rameix-Welti, M. A.; van der Werf, S.; Naffakh, N. *Virology* **2007**, *362*, 271.
26. Gabriel, G.; Dauber, B.; Wolff, T.; Planz, O.; Klenk, H. D.; Stech, J. *Proc. Natl. Acad. Sci. U.S.A.* **2005**, *102*, 18590.
27. Tarendeau, F.; Crepin, T.; Guilligay, D.; Ruigrok, R. W.; Cusack, S.; Hart, D. J. *PLoS Pathog.* **2008**, *4*, e1000136.
28. Kuzuhara, T.; Kise, D.; Yoshida, H.; Horita, T.; Murazaki, Y.; Nishimura, A.; Echigo, N.; Utsunomiya, H.; Tsuge, H. *J. Biol. Chem.* **2009**, *284*, 6855.
29. Motoshima, K.; Ishikawa, M.; Sugita, K.; Hashimoto, Y. *Biol. Pharm. Bull.* **2009**, *32*, 1618.
30. Fenn, J. B.; Mann, M.; Meng, C. K.; Wong, S. F.; Whitehouse, C. M. *Science* **1989**, *246*, 64.
31. Baca, M.; Kent, S. B. H. *J. Am. Chem. Soc.* **1992**, *114*, 3992.
32. Yang, C. S.; Wang, X.; Lu, G.; Picinich, S. C. *Nat. Rev. Cancer* **2009**, *9*, 429.
33. Song, J. M.; Lee, K. H.; Seong, B. L. *Antiviral Res.* **2005**, *68*, 66.
34. Morris, G. M.; Goodsell, D. S.; Halliday, R. S.; Huey, R.; Hart, W. E.; Belew, R. K.; Olson, A. J. *J. Comput. Chem.* **1998**, *19*, 1639.
35. Nakamura, Y.; Oda, K.; Nakada, S. *J. Biochem.* **1991**, *110*, 395.

36. Mullis, K. B.; Faloona, F. A. *Methods Enzymol.* **1987**, *155*, 335.
37. Studier, F. W.; Moffatt, B. A. *J. Mol. Biol.* **1986**, *189*, 113.
38. Janknecht, R.; de Martynoff, G.; Lou, J.; Hipskind, R. A.; Nordheim, A.; Stunnenberg, H. G. *Proc. Natl. Acad. Sci. U.S.A.* **1991**, *88*, 8972.
39. Taub, M.; Saier, M. H., Jr. *Methods Enzymol.* **1979**, *58*, 552.
40. Hierholzer, J. C.; Killington, R. A. *Virology Methods Manual*; Mahy, B. W. J., Kangro, H. O., Eds.; Academic Press Limited: London, 1996; Chaper 2, pp 35–37.